Modeling the dynamics of fine dust fraction in the surface layer of the atmosphere

Egor Savin[1], *Asvar* Akhmedov[2], and *Alexander* Khoperskov[1*]

[1]Volgograd State University, 100, Prospect Universitetsky, Volgograd, 400062, Russia
[2]Volgograd State Technical University, 28, Lenina prosp., Volgograd, 400005, Russia

Abstract. We investigated the operating conditions of excavator equipment, leading to unsteady dynamics of dust far from the pollution source. Wind transport of dust takes into account the non-uniform vertical wind profile. Diffusion movement is also determined by the inhomogeneous coefficient of turbulent diffusion with a nonmonotonic dependence on height. The Earth's surface is given by a digital elevation model, which allows calculations for a specific area with complex topography. Vertical inhomogeneities of wind and turbulence significantly change the nature of the spatial distributions of dust particles. Our approach makes it possible to determine changes in the disperse composition of particles with distance from the dust source.

1 Introduction

Studies of the dynamics of various aerosols types are extremely multifaceted and affect a wide range of human society problems from production and global climate change to the spread of the COVID-19 pandemic [1-3]. Dust propagation modeling for environmental applications requires high-quality models of the atmospheric surface layer due to complex air movements [4-5]. Similar problems arise when describing the motion of suspended particles in water bodies [6-8].

Dust is an important factor in atmospheric pollution due to both natural sources and anthropogenic factors [9]. The latter include construction and road works. Non-road construction equipment can be a significant non-stationary source of dust particles [10]. Dust can spread over very long distances, and the vertical inhomogeneities of the wind and air turbulence can greatly affect the distribution of these pollutants in space and time [11-12]. Dust from earthworks has a negative impact on human health, causing diseases of the upper and lower respiratory tract [13-14]. This danger is exacerbated in the case of PM10 and PM2.5 dust particles, which are long-lived components in the atmosphere. The aim of our work is to determine the conditions under which the non-stationary nature of dust pollution persists at large distances from a working excavator.

* Corresponding author: khoperskov@volsu.ru

2 Materials and methods

Model and simulation conditions.

Observations show an increase in wind speed $U_0^{(w)}$ with height [15-16], which is better approximated by a power law to ~ 150 m than by a logarithmic law, so we use the formula

$$U_0^{(w)}(z) = U_{01}^{(w)}\left(z / z_1^{(w)}\right)^{m_H} \quad (1)$$

Where $U_{01}^{(w)}$ is the wind speed at $z_1^{(w)}$, m_H is the Hellmann (or friction) coefficient. The exponent m_H in (1) is an empirical parameter and depends on the terrain (roughness of the underlying surface), atmospheric stratification and turbulence, and even wind speed [17, 18]. Therefore, there is a large uncertainty in its choice ($m_H = 0.15 - 1$) and the condition $m_H = 1/7$ is accepted for even surfaces [16, 19-21]. The inverse relationship between m_H and wind speed leads to a strong decrease in the Hellmann coefficient at $U_0^{(w)} \geq 8$ m/sec.

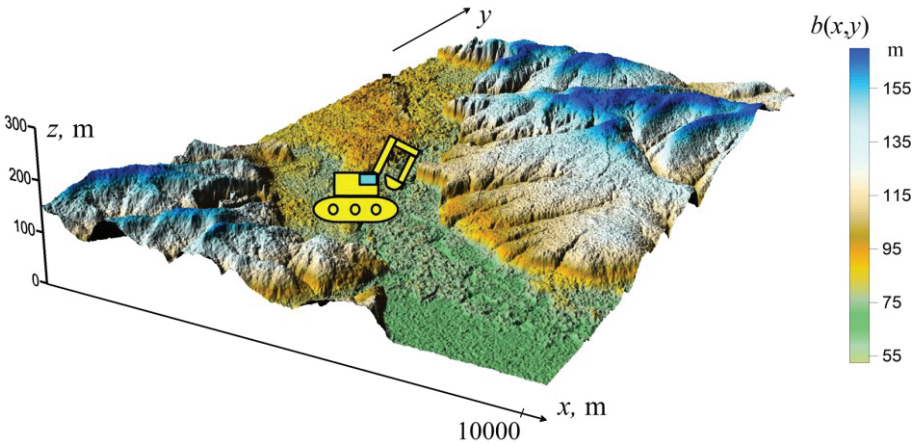

Fig. 1. An example of using a digital elevation model to set boundary conditions on the Earth's surface. The position of the dust source (excavator) is shown symbolically.

The surface of the Earth in the computational domain may not be flat and is given in our model by the topography $z = b(x, y)$ in the form of a heights matrix (Figure 1). The digital elevation model $b(x, y)$ allows you to conduct computational experiments for a real landscape with georeferencing within the framework of the developed Digital Hydrological Landscape Model, which sets the boundary conditions for dust adhesion at the lower boundary of the computational domain. In this case, the profiles of the wind speed and diffusion coefficient are recalculated so that these characteristics are equal to zero on the surface $z = b(x, y)$.

The movement of impurities in the air is determined by a diffusion type equation with sources [3-4, 9, 22]

$$\frac{\partial \rho}{\partial t} + \nabla\left(\rho \mathbf{U}^{(w)}\right) = \nabla\left(D^{(turb)}(\nabla\rho)\right) + q(x,y,z,t) + w_g \frac{\partial \rho}{\partial z} \tag{2}$$

Where ρ is the dust mass density ([ρ] = kg · m $^{-3}$), q is the non-stationary source that determines the distribution of the rate of dust ingress during construction work ([q] =kg · m $^{-3}$ sec $^{-1}$), w_g is the effective velocity of the particles falling, determined by the balance of the gravitational force and the Stokes force. The value of w_g depends on the size of the dust particle and the properties of the gaseous medium:

$$w_g = g\frac{(d^{(d)})^2}{18\mu}\left(\mathrm{c}^{(d)} - \mathrm{c}^{(a)}\right) \tag{3}$$

Where g = 9.8 m · sec $^{-2}$, $d^{(d)}$ is the spherical dust particle diameter, μ is the dynamic viscosity of air, $\mathrm{c}^{(d)}$ is the dust particle density, $\mathrm{c}^{(a)}$ is the air density, which can be neglected compared to $\mathrm{c}^{(d)}$. The function q determines the operating mode of an arbitrary number of sources ($L^{(s)}$), each of which can be non-stationary and is given by the coordinates:

$$q(\mathbf{r},t) = \sum_{\ell}^{L^{(s)}} q_{\ell}(\mathbf{r},t) \qquad Q = \int_{V^{(gen)}} q(\mathbf{r},t)dV \tag{4}$$

Where the function q_ℓ characterizes the ℓ -th source, Q is the total rate of dust entry into the volume $V^{(gen)}$ (Figure 1).

We also use a rather universal turbulent viscosity profile with two free parameters [15, 22-23]

$$D^{(turb)}(z) = \frac{\sqrt{e}D_{\max}^{(turb)}}{z_{\max}^{(turb)}} z \cdot \exp\left[-0.5\left(\frac{z}{z_{\max}^{(turb)}}\right)^2\right] \tag{5}$$

Where $D_{\max}^{(turb)}$ is the maximum value of turbulent diffusion and $z_{\max}^{(turb)}$ is the corresponding height. This approach ensures that the maximum is reached at a third of the height of the atmospheric boundary layer. The quantity $D^{(turb)}$ characterizes rather small-scale turbulence [11, 15, 24-25].

The base model is defined by the following set of parameters: $z_{\max}^{(turb)} = 100$ m, $D_{\max}^{(turb)} = 3\,\mathrm{m}^2\,\mathrm{sec}^{-1}$, $z_1^{(w)} = 10\,\mathrm{m}$, $U_{01}^{(w)} = 5\,\mathrm{m}\cdot\mathrm{sec}^{-1}$, $m_H = 1/7$, the dimensions of the computational domain are $x_{\max} = 1000\,\mathrm{m}$, $y_{\max} = 500\,\mathrm{m}$, $z_{\max} = 128\,\mathrm{m}$. The dust source parameters are the position $\vec{r}_Q = \{x_Q, y_Q, z_Q\}$, the power $Q_{av}^{(d)}$, the period τ_Q and

the duration of the emission dust T_Q. We vary the wind speed $U_{01}^{(w)}$, dust diameter, power and time characteristics of the dust source, their localization, number of sensors, etc. We use GPU parallel computing software based on CUDA technology.

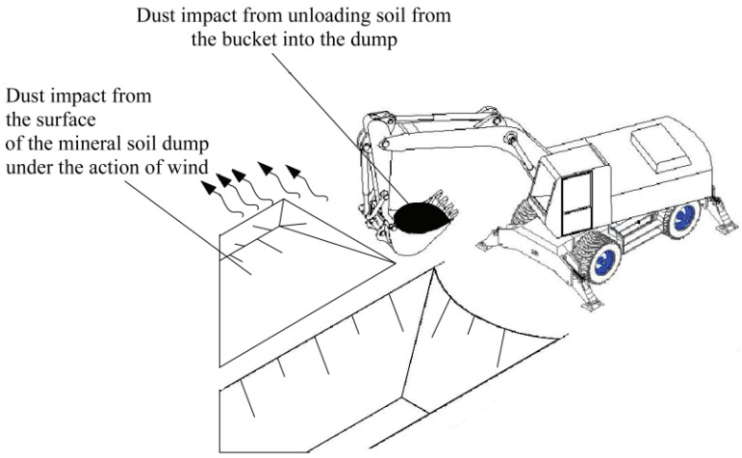

Fig. 2. We consider non-stationary sources of dust caused by the operation of an excavator.

The input data for numerical simulation of dust movement include its dispersed composition and are determined experimentally using SPOTEXPLORER 2018. The dispersed composition of particles was determined in a dust cloud according to the method in [26].

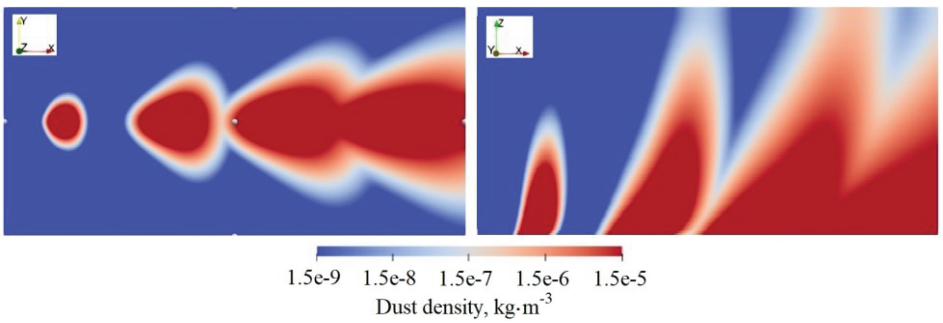

Fig. 3. General pattern of dust density distributions in two perpendicular sections.

3 Results and Discussion

Peculiarities of Dust Dynamics.

The peculiarity of the vertical profile of turbulent diffusion at high heights ($z > 200$ m) has little effect on rather heavy dust particles with a diameter of $d > 10$ micrometers, since the main fraction is inside the layer $z < z_{\max}^{(turb)}$. The lightest particles ($d^{(d)} < 2\mu$m) are transported predominantly at high heights above the $z_1^{(w)}$ layer due to vertical inhomogeneity of wind and diffusion coefficient.

Figure 3 shows a typical example of dust mass density distribution for the base model. The left panel demonstrates $\rho(x, y)$ at height $z = 2$ m. The distribution of dust in the vertical plane is shown in the right panel. The unsteady operation of the dust source is clearly visible. Inhomogeneous propagation occurs in various directions due to the dependence of wind and diffusion on spatial coordinates. The influence of a non-stationary source is preserved up to distances of about 1 km.

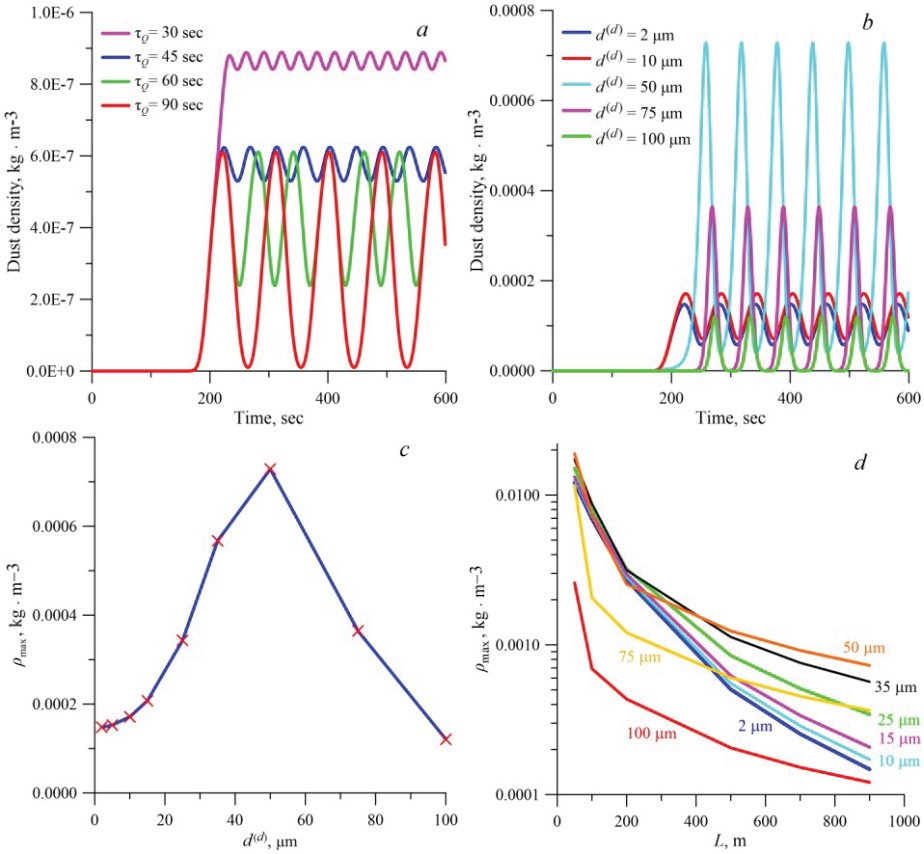

Fig. 4. Time dependences of dust density at a distance of 900 m for different periods of dust emission (*a*), particle diameters (*b*). Dependences of the maximum dust density $\rho_{\max}$ on the dust particle diameter (*c*), distance to the source for different parameters (*d*).

We characterize non-stationarity by the parameter $\delta_c = 2(\rho_{\max} - \rho_{\min})/(\rho_{\max} + \rho_{\min})$, which decreases with distance from the source and strongly depends on the operation mode of the excavator. Figure 4*a* shows the results for the base model, where δ_c is less than 0.2 even at $\tau_Q <$ 50 sec. Note that the measurement error of the aerosol particle counter (Lighthouse Handheld) is 20 percent. Increasing the period of the source operation to 90 sec qualitatively changes the pattern of pollution at large distances, where the sensors fix strongly non-stationary solutions (red line in Figure 4*a*).

Let us consider the measurement results of the sensor located at a distance of 900 m from the source at a height of $z = 2$ m in more detail. Figure 4*b* shows the time dependence of dust density for five dust particle diameters ($d^{(d)} = 2, 10, 50, 75, 100 \mu$m). The

nonmonotonic dependence of the dust density on the particle diameter seems to be important, which is due to the vertical inhomogeneity of the atmospheric parameters and the strong dependence of the precipitation rate on the size of the dust grain (Figure 4*c*). The dust concentration increases with increasing power of the source, retaining the periodic character. The law of decreasing the maximum density $\rho_{\max}$ differs for particles of different diameters (Figure 4*d*). There is a non-monotonic dependence of the concentration on the diameter at different distances from the emission source.

4 Conclusion

The numerical model has been created to study the dynamics of dust from road construction equipment, which makes it possible to perform computational experiments for non-stationary operation modes. We take into account vertically distributed profiles of wind speed and turbulent diffusion coefficient. Our software allows us to use a digital terrain model of a real territory, including buildings in settlements, as boundary conditions on the Earth's surface. We have studied the conditions under which non-stationary dust sources lead to strong fluctuations in pollution density over long distances.

The size of dust particles is a critical parameter. The dust concentration of different diameters in the surface layer of the atmosphere is nonmonotonic and strongly depends on the ratio of wind parameters, atmosphere turbulent state and nonstationary source. There is a critical value of the diameter ($d_{crit}^{(d)}$), which makes the main contribution to the mass density of dust pollution during the operation of the excavator or bulldozer equipment. The value of $d_{crit}^{(d)}$ is very sensitive to the state of the atmosphere and the operation mode of the equipment. These results require clarification when applying environmental standards that define dust pollution.

Acknowledgement

The research was supported by the Russian Science Foundation (RSF project No. 23-71-00016, https://rscf.ru/project/23-71-00016/).

References

1. T.S. Sarin, V. Vinoj, D. Swain, K. Landu, E. Suhas, Front. Mar. Sci., **8**, 648566 (2021)
2. S. Woodward, A. Sellar, Y. Tang, M. Stringer, A. Yool, E. Robertson, A. Wiltshire, Atmospheric Chemistry and Physics, **22**, 14503-14528 (2022)
3. E.S. Savin, A.S. Kuzmich, J.V. Startseva, A.V. Titov, A.V. Khoperskov, AIP Conference Proceedings, **2410**, 020023 (2021)
4. F. Ferraro, S. Gierth, S. Salenbauch, W. Han, C. Hasse1, Phys. Fluids, **34**, 075121 (2022)
5. S.V. Kakareka, S.V. Salivonchyk, Russ. Meteorol. Hydrol., **46**, 331–340 (2021)
6. A.I. Sukhinov, A.E. Chistyakov, V.V. Sidoryakina, S.V. Protsenko, A.M. Atayan, Mathematical Physics and Computer Simulation., **24**, 2, 38-53 (2021)
7. J.J. Monaghan, European Journal of Mechanics – B/Fluids., **79**, 454-462 (2020)
8. S.S. Khrapov, A.V. Khoperskov, Lobachevskii Journal of Mathematics., **41**, **8**, 1475-1484 (2020)

9. B. Cvetkovic, P. Dagsson-Waldhauserov, S. Petkovic, O. Arnalds, F. Madonna, E. Proestakis, A. Gkikas, A.V. Vimic, G. Pejanovic, M. Rosoldi, D. Ceburnis, V. Amiridis, L. Lis, S. Nickovic, J. Nikolic, Atmosphere, **13**, 1345 (2022)
10. B. Wu, W. Wang, Z. Yao, K. Xuan, Z. Wu, X. Shen, X. Li, H. Zhang, Y. Xue, X. Cao, X. Hao, Q. Zhou, Sci. Total Environ, **853**, 158601 (2022)
11. C. Tong, K.X. Nguyen, J Atmos Sci, **72**, 4337-4348 (2015)
12. A.C. Monin, A.M. Obukhov, Tr. Akad. Nauk SSSR Geophiz. Inst., **24**, 163-187 (1954)
13. Q. Luo, L. Huang, X. Xue, Z. Chen, F. Zhou, L. Wei, J. Hua, Journal of Building Engineering, **44**, 103186 (2021)
14. D. Cheriyan, J. Choi, Journal of Cleaner Production, **254**, 120077 (2020)
15. R. Frehlich, IOP Conference Series: Earth and Environmental Science, 1, 012017 (2008)
16. E.A. Kiseleva, E.N. Kiselev, A.V. Pogorelov, Proceedings of the International conference “InterCarto. InterGIS”, **21**, 266-273 (2015)
17. Y. Wu, Q. Li, G. Li, B. He, L. Dong, H. Lan, Earth and Space Sci., 9, e2021EA002095 (2022)
18. G. Gualtieri, S. Secci, Renew. Energ., **43**, 183-200 (2012)
19. H.L. Wegley, J.V. Ramsdell, M.M. Orgill, R.L. Drake, Siting Handbook for Small Wind Energy Conversion Systems (Battelle Pacific Northwest Labs, United States, 1980)
20. V.V.N. Kishore, Renewable Energy Engineering and Technology: A Knowledge Compendium (TERI Press, New Delhi, 2008)
21. C.G. Justus, A. Mikhail, Geophys. Res. Lett., **3**, 251–264 (1976)
22. M.A. Davydova, S.A. Zakharova, N.F. Elansky, Dokl. Earth Sci., **490**, 92-96 (2020)
23. B. Grisogono, L. Kraljevic, A. Jericevic, Q J R Meteorol Soc, **133**, 2133–2136 (2007)
24. J.J. O’Brien, J Atmos Sci, **27**, 1213-1215 (1970)
25. A.S. Monin, A.M. Yaglom, Statistical Fluid Mechanics, Volume I: Mechanics of Turbulence (Dover Publications) (2007)
26. A.I. Evtushenko, A.A. Sakharova, V.O. Kharlamov, V.N. Azarov, IOP Conference Series: Materials Science and Engineering, **913**, 032047 (2020)